

DIRECT CONTROL OF THE STATOR FLUX AND TORQUE OF THE THREE-PHASE ASYNCHRONOUS MOTOR USING A 2-LEVEL INVERTER WITH SINUSOIDAL PULSE WIDTH MODULATION

¹LOUBNA LAZRAK, ²SOUKAINA EL DAOUDI, ³CHIRINE BENZAZAH,

⁴MUSTAPHA AIT LAFKIH

^{1,2,3,4}Laboratory of Automatic, Energy Conversion and Microelectronics (LACEM), Department of electrical engineering, Faculty of Sciences and Technology, University of Sultan Moulay Slimane, Beni Mellal, Morocco

E-mail: ¹lazrakfst@yahoo.fr, ²soukainaeldaoudi@gmail.com, ³ch.benzazah@gmail.com, ⁴aitlafkihmustapha@yahoo.fr

ABSTRACT

This paper presents a direct control of the stator flux and torque of a three-phase asynchronous motor fed via a conventional voltage inverter to PWM pulse width modulation (sinus-triangle). This command uses PI type controllers, their parameters are determined from two control methods: The identification and the optimal symmetry criterion. The two-phase voltages obtained at the output of the PI regulators are compared with high frequency triangular signals to develop the control of the IGBTs of the inverter. The performance of the asynchronous motor control is verified by simulations under MATLAB / SIMULINK.

Keywords: *Direct Torque Control, Direct Flux Control, Induction Motor, PI Controller, Pulse Width Modulation, 2-Level Inverter, Optimal Symmetry Criterion*

1. INTRODUCTION

The increasingly development of efficient technologies for static converters has made it possible to extend the field of application of electrical machines in industry [1], among these electrical machines, DC motors were the first to benefit from these researches; however the presence of the collector limits their operation in the field of great powers. AC motors take over in the field of high power and especially the asynchronous squirrel cage motor which is highly valued for its robustness, high efficiency and low maintenance. Associated with a suitable static converter, such as cyclo-converters or inverters, the asynchronous motor can operate with a variable speed while controlling its startup. In order to improve the performance of the machine, a variety of control strategy was born, scalar control and vector control. Scalar control consists mainly of two types; constant V/F control and scalar control of the stator current, while vector control strategies are very varied and each of the control methods has characteristics which define it and which is suitable for a given application [2]. Oriented flow control

(FOC) is a vector strategy that assigns high performance to asynchronous motors by decoupling their variables; but it uses a rather high number of regulation loops which leads to a slow dynamics of the flux, on the other hand, its control structure depends on the rotor parameters which vary [3]. With direct torque control (DTC), which was first proposed by I. Takahashi and T. Noguchi [4], it is possible to directly control the stator flux and torque by selecting the appropriate state of the inverter [4] from a table called "optimal switching table". The choice of the state of the inverter is based on the outputs of the hysteresis regulators of the stator flux and the torque knowing the angle of the flow of the stator. Known for its simple structure and good performance, the DTC control has some disadvantages, such as variable switching frequency operation, which favors current and torque ripples, noise, and large switching losses [5]. This work presents direct flux and torque control using sinusoidal PWM and PI controllers. This control strategy has a structure independent of the variable parameters of the rotor, easily implemented in practice and which requires no current loop, it also has the advantage of good torque control even

at low speed while working with a constant switching frequency, which greatly reduces switching losses.

2. RELATED WORK

The induction motor was invented in 1888 by Nikola Tesla [17]. Dolivo Dobrowolski extended its structure in 1890 which is known as squirrel-cage motor [18]. In the past decades, DC motors have been extensively applied for modern industrial applications. However, their disadvantages prevent implementation of high performance drives. Due to the advantages of IM compared to DC and synchronous motors such as robust construction, low cost and maintenance, numerous attempts have been made to apply it in modern applications. In recent years, researchers have paid attention to develop the strategy of control for this type of motors due to its wide use [19], specially the vector control strategies such as FOC which was presented for the first time in 1971 by F. Blaschke [20] and DTC who is known for its fast torque and flux responses [4], but as this method involves sector determination and angle calculation of voltage vector it makes it complicated and it consumes more memory with a wide range of torque and flux ripples, so to surpass the high ripples in torque and flux signals, R.TOUFOUTI proposed two approach intelligent techniques of improvement of Direct Torque Control (DTC) of Induction motor such as fuzzy logic (FL) and artificial neural network (ANN), applied in switching select voltage vector [21]. However, this strategy keeps the switching frequency variable which keeps several disadvantages. A modulation-based DTC strategy is suggested and been developed by many researchers, H. ABU-RUB has dealt with this strategy and proposed a Simple DTC-SVM scheme for induction motor drives with PI controllers [22]. Since the PI controller is the most common solution to practical control problems, it is necessary to choose among the various existing tuning techniques to obtain the desired performance depending on the dynamics of the process and the way the controller is being applied. C. BAJRACHARYA discussed the tuning techniques of converter controllers, the results show that the tuning according to symmetric optimum provides high proportional gain and low integral time constant, which results in fast response as well as strong rejection of disturbance [9]. So, the purpose of this paper is to gather the most advantageous techniques to control the induction motor by treating the use of pulse width modulation in the direct control of induction motor's torque and flux based on PI regulators tuned by optimal

symmetry criterion, aiming to obtain a stable performance and reduced torque/flux ripples.

3. MODELING OF THE ASYNCHRONOUS MOTOR IN THE TWO-PHASE REFERENCE

The differential equations of the rotor and stator electric circuits can be put into a matrix form, connecting the voltages of each of the stator or rotor coils $[V_{r,s}^{a,b,c}]$ with currents $[i_{r,s}^{a,b,c}]$ and flows $[\varphi_{r,s}^{a,b,c}]$ through the equation:

$$[V_{r,s}^{a,b,c}] = [R_{r,s}] [i_{r,s}^{a,b,c}] + \frac{d}{dt} [\varphi_{r,s}^{a,b,c}] \quad (1)$$

In the particular case of the asynchronous squirrel cage motor, the voltage vector $[V_r]$ is zero. The flux vector $[\varphi_{a,b,c}^{r,s}]$ depends on both the rotor currents $[i_r]$ and the stator currents $[i_s]$:

$$[\varphi_{a,b,c}^{r,s}] = [L_{ss,rr}] [i_{a,b,c}^{r,s}] + [M_{sr}] [i_{a,b,c}^{s,r}] \quad (2)$$

$[L_{ss,rr}]$ is the inductance matrix (rotor and stator) containing self, magnetization, leakage and mutual inductances [6].

$[M_{sr}]$ is the matrix of mutual inductances between stator and rotor.

Electric equations

The equations of voltages and currents of the three-phase asynchronous motor in the (d, q) frame are:

$$\begin{cases} V_{ds} = R_s I_{ds} + \frac{d\varphi_{ds}}{dt} - \omega_s \varphi_{qs} \\ V_{qs} = R_s I_{qs} + \frac{d\varphi_{qs}}{dt} + \omega_s \varphi_{ds} \\ 0 = R_r I_{dr} + \frac{d\varphi_{dr}}{dt} - \omega_g \varphi_{qr} \\ 0 = R_r I_{qr} + \frac{d\varphi_{qr}}{dt} + \omega_g \varphi_{dr} \end{cases} \quad (3)$$

$$\begin{cases} I_{ds} = \frac{1}{\sigma L_s} \varphi_{ds} - \frac{M}{\sigma L_r L_s} \varphi_{dr} \\ I_{qs} = \frac{1}{\sigma L_s} \varphi_{qs} - \frac{M}{\sigma L_r L_s} \varphi_{qr} \\ I_{dr} = -\frac{M}{\sigma L_s L_r} \varphi_{ds} + \frac{1}{\sigma L_r} \varphi_{dr} \\ I_{qr} = -\frac{M}{\sigma L_s L_r} \varphi_{qs} + \frac{1}{\sigma L_r} \varphi_{qr} \end{cases} \quad \text{With: } \sigma = 1 - \frac{M}{L_s L_r} \quad (4)$$

With σ is the leakage or dispersion factor, ω_g is the slip frequency that is obtained from the equation below, where: ω_s (ω_r) is the stator (rotor) pulsation:

$$\omega_g = \omega_s - \omega_r \quad (5)$$

φ_{ds} (φ_{dr}) and φ_{qs} (φ_{qr}) are the stator fluxes (rotor fluxes) along the axis d and q respectively [7], the equations (6) express these fluxes as a function of mutual inductances, stator and rotor inductances. These expressions are taken from the electrical equations of currents.

$$\begin{cases} \varphi_{ds} = L_s I_{ds} + M I_{dr} \\ \varphi_{qs} = L_s I_{qs} + M I_{qr} \\ \varphi_{dr} = L_r I_{dr} + M I_{ds} \\ \varphi_{qr} = L_r I_{qr} + M I_{qs} \end{cases} \quad (6)$$

The leakage inductances of the stator and rotor are expressed according to the equation below:

$$L_{sl} = L_s - M, L_{rl} = L_r - M \quad (7)$$

The equivalent model of the asynchronous motor along the axes of the two-phase reference (d,q) is as follows:

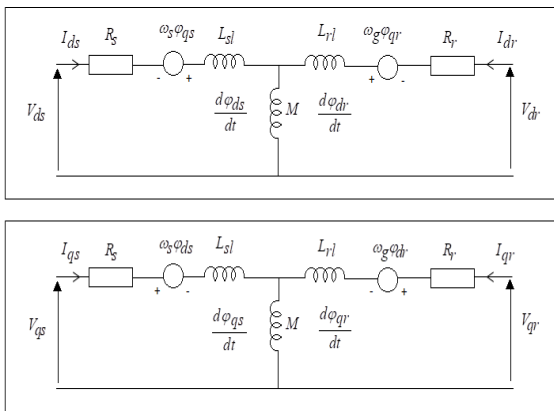


Figure 1. Equivalent Circuit of asynchronous motor in the (d,q) frame

Mechanical equation

$$J \frac{d\Omega}{dt} = C_e - C_r - f\Omega \quad (8)$$

Ω : Motor speed, J : Moment of inertia, f : Coefficient of friction and C_r : Load torque.

Expression of electromagnetic torque

$$C_e = \frac{3}{4} P (\varphi_{ds} I_{qs} - \varphi_{qs} I_{ds}) \quad (9)$$

With P is the number of pole pairs.

4. DIRECT CONTROL OF THE STATOR FLUX, TORQUE AND SPEED

To control the engine parameters; speed, torque and stator flux, the proposed control is based on PI controllers which improves the dynamics of the system while eliminating the static error between the estimated magnitudes and the references. The block diagram of the entire system is represented in Figure 2. The regulation is done according to three loops, two cascade loops to control the speed and the torque, the third one is for the stator flux control.

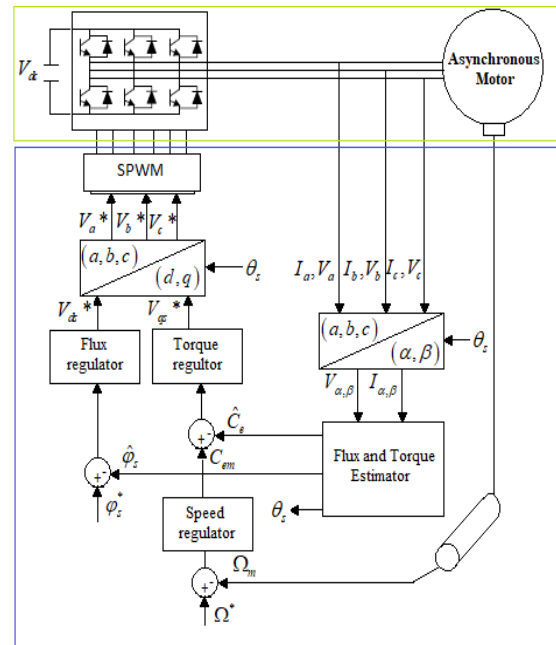


Figure 2. Block diagram of the system for direct control of torque and stator flux via a two-level inverter for an asynchronous motor

4.1 Speed Control

Asynchronous motor speed control is frequently implemented in a large number of applications, for this reason, research gives great importance to speed control since the output of the speed loop is also a reference for other control loops. The process equation used for this control is:

$$J \frac{d\Omega}{dt} = C_e - C_r - f\Omega \quad (10)$$

The regulation is based on a PI regulator in the form:

$$G_{PI}(s) = \frac{K(1+\tau s)}{\tau s} \quad (11)$$

With: K and τ are respectively the proportional and integrator factors of the regulator. The block diagram of the speed control loop is shown in Figure 3.

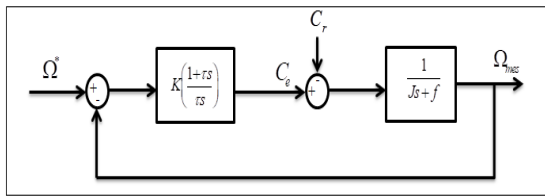


Figure 3. Mechanical Speed Control Loop

In the proposed control, we considered the current control block as a classical PI controller. For this, the dynamics of the current loop compared to that of the speed is neglected. Consider the load torque as a disturbance, the open loop function becomes:

$$G_{\Omega OL}(s) = \frac{\Omega_{mes}(s)}{\Omega^*(s)} = \frac{1}{Js+f} \left[K \left(\frac{1+\tau s}{\tau s} \right) \right] \quad (12)$$

The closed loop transfer function then becomes:

$$\Omega_{mes} = \frac{1}{Js+f} K \left(\frac{1+\tau s}{\tau s} \right) (\Omega^* - \Omega_{mes}) \quad (13)$$

Such:
$$\Omega_{mes} = \frac{Ks + \frac{K}{\tau}}{Js^2 + (K+f)s + \frac{K}{\tau}} \Omega^* \quad (14)$$

So:
$$G_{\Omega CL}(s) = \frac{\Omega_{mes}(s)}{\Omega^*(s)} = \frac{Ks + \frac{K}{\tau}}{Js^2 + (K+f)s + \frac{K}{\tau}} \quad (15)$$

With: Ω_{mes} and Ω* are respectively measured and reference speeds. The transfer function can be identified with a second-order system in the form [8] :

$$G(s) = \frac{1}{1 + 2\xi\tau_n s + \tau_n^2 s^2} \quad (16)$$

With: τ_n is the opposite of natural frequency of the system, ξ is the damping ratio. At each value of ξ, we can have an equivalent value of $\frac{t_{rp}}{\tau_n}$ with t_{rp} is the response time of the system. This allows setting the dynamics freely.

The resolution of this system involves the following identities:

$$\begin{cases} J\tau = \tau_n^2 \\ \frac{K}{K+f} \\ \frac{K+f}{K} \tau = 2\xi\tau_n \end{cases} \quad (17)$$

The bode diagram of the closed-loop transfer function shows stable operating limits with a maximum phase margin of 90.1°, occurring at the cutoff frequency of 32.5 rad/s (5.17 Hz).

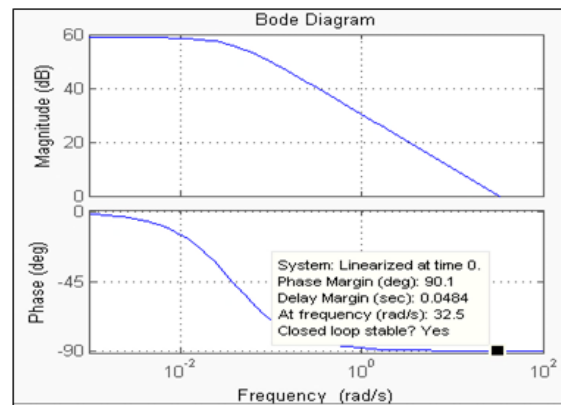


Figure 4. Bode diagram of the closed-loop transfer function of the speed controller

4.2 Flux Control

The synoptic shape of the closed loop of the stator flux with a PI regulator is shown in the figure below [9],[10].

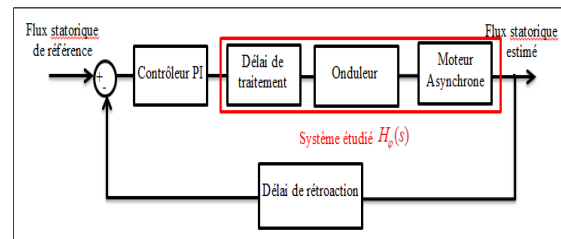


Figure 5. Block diagram of the closed loop of the stator flux control taking into account the delays of the process

It consists of a PI controller block; its transfer function is of the form:

$$G_{PI}(s) = K \left(\frac{1 + \tau s}{\tau s} \right) \quad (18)$$

With: K and τ are respectively the proportional gain and the integration time. The transfer function for the digital signal processing delay is presented in equation (19), where T_p is the processing/execution time of the algorithm:

$$G_{pd}(s) = \frac{1}{T_p s + 1} \quad (19)$$

The third block consists of the inverter model with a transfer function in the form:

$$G_{inv}(s) = \frac{1}{\tau_o s + 1} \quad (20)$$

With: τ_o is the dead time of the inverter.

The last block is the transfer function of the feedback filter which T_f the filter delay:

$$G_f(s) = \frac{1}{T_f s + 1} \quad (21)$$

Considering the equation of the direct stator voltage, the control will be described using the following equation:

$$V_{ds} = R_s I_{ds} + \frac{d\varphi_{ds}}{dt} - \omega_s \varphi_{qs} \quad (22)$$

By neglecting the voltage drop in the stator resistance R_s and since the quadrature component of the stator flux is zero ($\varphi_{qs} = 0$), the function between the stator flux and the direct stator voltage becomes linear such that:

$$G_\varphi(s) = \frac{\varphi_s(s)}{V_{ds}(s)} = \frac{1}{s} \quad (23)$$

The open-loop transfer function of this control system is written in the following form:

$$G_{\varphi OL}(s) = K \frac{1 + \tau s}{\tau s} \cdot \frac{1}{T_f s + 1} \cdot \frac{1}{\tau_o s + 1} \cdot \frac{1}{T_p s + 1} \cdot \frac{1}{s} \quad (24)$$

Since the sum of the small time constants which includes the static delay of the inverter (Dead Time) τ_o , execution time of the algorithm T_p and T_f the delay of the feedback filter is defined by:

$T_\varphi = T_f + T_p + \tau_o$, the transfer function in open loop will be written:

$$G_{\varphi OL}(s) = K \frac{1 + \tau s}{\tau s} \cdot \frac{1}{T_\varphi s + 1} \cdot \frac{1}{s} \quad (25)$$

The closed loop transfer function is written in the following form [9]:

$$G_{\varphi CL}(s) = \frac{\varphi_{sm}(s)}{\varphi_s^*(s)} = \frac{1 + \tau s}{1 + \tau s + \frac{\tau}{K} s^2 (T_\varphi s + 1)} = \frac{1 + \tau s}{1 + \tau s + \frac{\tau}{K} s^2 + \frac{\tau}{K} T_\varphi s^3} \quad (26)$$

With: φ_{sm} and φ_s^* are respectively the estimated and reference stator fluxes.

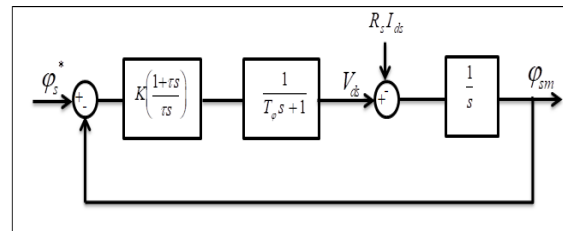


Figure 6. Stator flux control loop

For the design of the stator flux controller parameters, the optimum symmetry criterion is applied [11],[12],[2]. According to this criterion, the function which describes the studied system can be put in the general form:

$$H_\varphi(s) = \frac{K_o e^{-s\tau_o}}{s T_\sigma (1 + s T_\mu)} = \frac{1}{s (T_\sigma s + 1)} \quad (27)$$

With: K_o , T_μ , τ_o et T_σ are the parameters of the studied system. The inverter used is considered ideal, it allows to put $\tau_o = 0$ 'Dead time is zero'. The PI controller parameters are:

$$\begin{cases} K = \frac{T_\sigma}{2K_o(T_\mu + \tau_o)} \\ K = \frac{T_\sigma}{\tau \cdot 8K_o(T_\mu + \tau_o)^2} \end{cases} \quad (28)$$

In that case: $T_\mu = T_\varphi$, $T_\sigma = T_1 = 1$, $K_o = 1$

The bode diagram of the closed-loop transfer function shows stable operating limits with a maximum phase margin of 36.9°, occurring at the cutoff frequency of $1 \cdot 10^5$ rad / s (15.915 KHz).

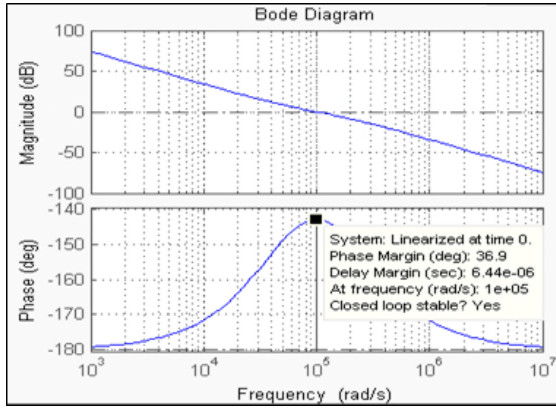


Figure 7. Bode diagram of the closed-loop transfer function of the flux controller tuned with the optimal symmetry criterion

4.3 Torque Control

The block diagram of the closed torque loop is shown in Figure 8 [9],[10].

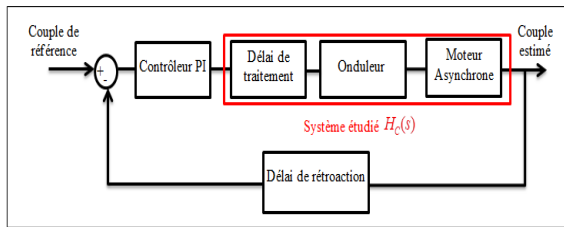


Figure 8. Closed loop torque control block diagram taking into account process delays

It consists of a PI type controller block; its transfer function is of the form:

$$G_{PI}(s) = K \left(\frac{1 + \tau s}{\tau s} \right) \quad (29)$$

With: K and τ are respectively the proportional gain and the integration time. The transfer function for the digital signal processing delay is presented in equation (30), where T_p is the processing/execution time of the algorithm:

$$G_{pd}(s) = \frac{1}{T_p s + 1} \quad (30)$$

The third block consists of the inverter model with a transfer function in the form:

$$G_{inv}(s) = \frac{1}{\tau_o s + 1} \quad (31)$$

With: τ_o is the dead time of the inverter.

The last block is the transfer function of the feedback filter which T_f is the filter delay:

$$G_f(s) = \frac{1}{T_f s + 1} \quad (32)$$

The equation of the electromagnetic torque:

$$C_e = \frac{3}{4} P (\varphi_{ds} I_{qs} - \varphi_{qs} I_{ds}) \quad (33)$$

Taking into account that the quadrature component of the stator flux is zero ($\varphi_{qs} = 0$), this makes it possible to have a linear function between the torque and the quadrature stator current:

$$C_e = \frac{3}{4} P (\varphi_{ds} I_{qs}) \quad (34)$$

Since the torque control proposed in this paper consists in extracting the stator voltage in quadrature, equation (34) can be rewritten using current expression as a function of the quadrature voltage (3):

$$I_{qs} = \frac{1}{R_s} [V_{qs} - \omega_s \varphi_{ds}] \quad (35)$$

$$C_e = \frac{3}{4} \frac{P}{R_s} \varphi_{ds} [V_{qs} - \omega_s \varphi_{ds}] \quad (36)$$

Equation (36) shows that the coupling between torque and flux is omitted, since the quantity is considered a disturbance and the direct component of the flux is a constant, hence the following transfer function:

$$G_C(s) = \frac{C_e(s)}{V_{qs}(s)} = \eta_t \quad (37)$$

With: $\eta_t = \frac{3}{4} \frac{P}{R_s} \varphi_{ds}$

The open loop transfer function then becomes:

$$G_{COL}(s) = K \frac{1 + \tau s}{\tau s} \cdot \frac{1}{T_p s + 1} \cdot \eta_t \quad (38)$$

The closed loop transfer function is written in the following form [9]:

$$G_{CL}(s) = \frac{C_{em}(s)}{C_e^*(s)} = \frac{1+\tau s}{1+\tau s + \frac{\tau}{K\eta} s(T_\phi s+1)} = \frac{1+\tau s}{1 + \left(\tau + \frac{\tau}{K\eta}\right) s + \frac{\tau}{K\eta} T_\phi s^2} \quad (39)$$

With: C_{em} and C_e^* are respectively estimated and reference torques.

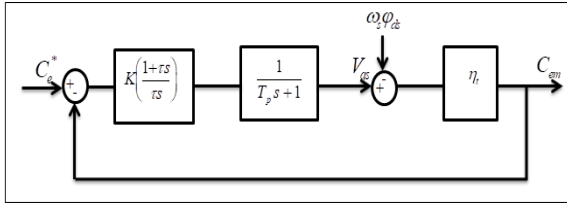


Figure 9. Torque control loop

The criterion used in the control of the torque is that of Symmetry optimal [11],[12],[2], according to this criterion, the function which describes the studied system can be put in the general form:

$$H_C(s) = \frac{K_0 e^{-s\tau_0}}{1+sT_\mu} = \frac{\eta_t}{(T_\phi s+1)} \quad (40)$$

With: K_0, T_μ et τ_0 are the parameters of the studied system. We considered that the inverter used is ideal, it allows to put $\tau_0 = 0$ 'Dead time is zero' and the damping factor $\xi = 1$. The PI controller parameters are:

$$\begin{cases} K=1 \\ K = \frac{(1+K_0)^2}{4\xi^2 T_\mu K_0} \end{cases} \text{ With: } T_\mu = T_\phi, K_0 = \eta_t \quad (41)$$

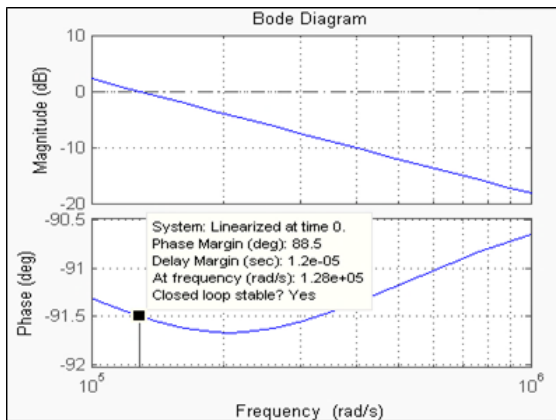


Figure 10. Bode diagram of the closed-loop transfer function of the torque controller tuned with the optimal symmetry criterion

The bode diagram of the closed-loop transfer function shows stable operating limits with a maximum phase margin of 88.5°, occurring at the cutoff frequency of 1.28×10^5 rad / s (20.371 KHz).

5. TORQUE AND FLUX ESTIMATOR

From the point of view of control theory, the performance of a feedback control system relies on the accuracy of the feedback signal. For accurate and robust control characteristics, the most accurate signal must be selected as the feedback signal. In our case, the control used is based on an estimation of the torque and the stator flux, the latter can be evaluated more precisely than the rotor flux which has a certain limitation of performance due to the effects of “detuning”. A major cause of “detuning” is the variation of the leakage inductance that is used in the estimation of the rotor flux [13]. The feedback parameters can be evaluated in the reference (α, β) and with the equations below:

$$\begin{cases} \hat{\phi}_{s\alpha} = \int_0^t (V_{s\alpha} - R_s I_{s\alpha}) dt \\ \hat{\phi}_{s\beta} = \int_0^t (V_{s\beta} - R_s I_{s\beta}) dt \end{cases} \quad (42)$$

$$\hat{\phi}_s = \hat{\phi}_{s\alpha} + j\hat{\phi}_{s\beta} \quad (43)$$

The position and the modulus of the stator flux vector are calculated as follows:

$$\bar{\phi}_s = \sqrt{\hat{\phi}_{s\alpha}^2 + \hat{\phi}_{s\beta}^2}; \theta_S = \text{arctg}\left(\frac{\hat{\phi}_{s\beta}}{\hat{\phi}_{s\alpha}}\right) \quad (44)$$

The motor electromagnetic torque estimator is based on the torque equation according to the estimated fluxes and the stator currents measured according to equation (45):

$$\hat{C}_e = \frac{3}{4} P (\hat{\phi}_{\alpha s} I_{\beta s} - \hat{\phi}_{\beta s} I_{\alpha s}) \quad (45)$$

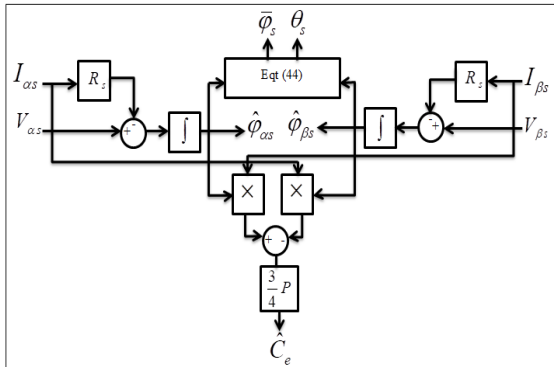


Figure 11. Stator flux and torque estimators in the (α, β) frame

6. SPWM MODULATION OF A 2-LEVEL INVERTER

6.1 Three-phase two-level inverter

In the structure of the two-level three-phase inverter fed by a DC source V_{dc}, there are three arms each composed of 2 switches $K'_x, K_x(1,2,3)$ with an antiparallel protection diode for each bipolar transistor insulated gate 'IGBT'. These diodes provide freewheeling. The three middle points of each arm A, B and C feed the three-phase machine.

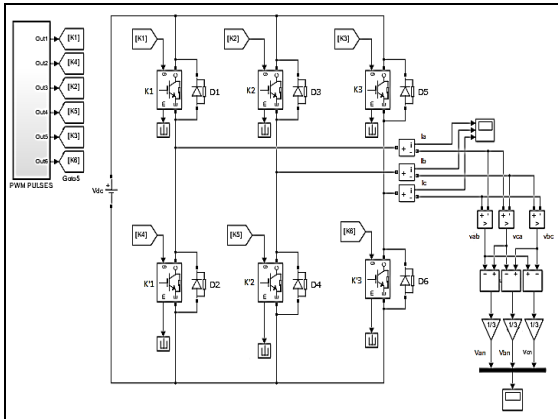


Figure 12. Three-phase two-level inverter

Table 1 below explains the switching states of the transistors:

- 'P' indicates that the voltage across the inverter is positive.
- 'B' indicates that the voltage across the inverter is zero because of the conduction of the lower part.

Table 1: Output status of each arm of the 2-level inverter.

	K'_x	K_x	Phase voltage	Leg status
1	ON	OFF	V _{dc}	P
2	OFF	ON	0	B

Due to the three active branches, three switching functions s_a, s_b and s_c are associated with the three-phase complete-bridge inverter. The line-to-line and line-to-neutral output voltages are given by:

$$\begin{bmatrix} V_{an} \\ V_{bn} \\ V_{cn} \\ V_{ab} \\ V_{bc} \\ V_{ca} \end{bmatrix} = \begin{bmatrix} V_{dc} & 2 & -1 & -1 \\ -1 & 2 & -1 \\ -1 & -1 & 2 \\ 1 & -1 & 0 \\ 0 & 1 & -1 \\ -1 & 0 & 1 \end{bmatrix} \begin{bmatrix} s_a \\ s_b \\ s_c \end{bmatrix} \quad \text{Avec: } s_a = \begin{cases} 1 \text{ si } K_1 = \text{ON et } K'_1 = \text{OFF} \\ 0 \text{ si } K_1 = \text{OFF et } K'_1 = \text{ON} \end{cases} \quad (45)$$

Each line-to-line voltage can take three values: V_{dc}, 0 and -V_{dc}, and each line-to-neutral voltage can take: $\frac{2}{3}V_{dc}, \frac{1}{3}V_{dc}, 0, -\frac{1}{3}V_{dc}$ et $-\frac{2}{3}V_{dc}$. In PWM mode, the maximum voltage gain is 1, ie the maximum attainable peak value of the fundamental line voltage is equal to the DC supply voltage [2].

6.2 PWM pulse width modulation control (sine-triangle):

The most common and popular technique among interspecific PWM approaches is the sinusoidal pulse width modulation (sine-triangle) [14],[15]. This technique is based on the comparison of a low frequency reference sine wave with a higher frequency triangular wave to reduce the harmonic rate (Figure 14) [16]. Using these two signals as comparator inputs, the output will be a two-level square signal that determines the switching times (Figure 13). Characteristics of this modulation are:

- The modulation rate:

It is defined as the ratio of the frequency of the carrier and the modulating wave.

$$t_m = \frac{f_p}{f_m} \quad (43)$$

To avoid low order harmonics, this ratio t_m must be greater than 20 (commonly accepted rule of thumb).

- The modulation index:

Also called the adjustment coefficient, it is the ratio of the amplitudes of the modulating signal and the carrier.

$$m = \frac{\hat{V}_m}{\hat{V}_p} \quad (44)$$

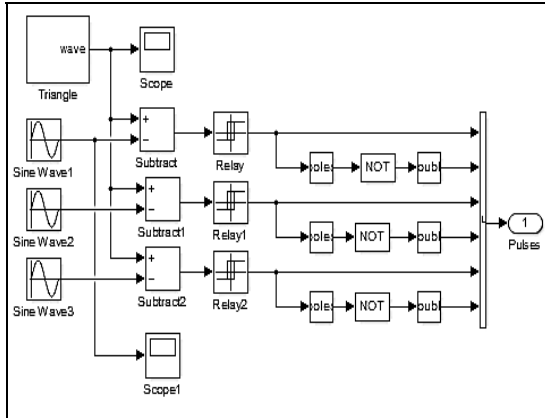


Figure 13. PWM technique using a sinusoidal and triangular signal

Figure 14 shows the signals and pulses of the control switches of the SPWM (sine-triangle) for a 2-level inverter.

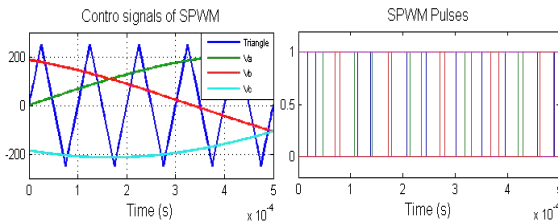


Figure 14. The six pulses resulting from the SPWM (sine-triangle)

7. SIMULATION RESULTS

- Switching on and starting unladen:

In order to prove the performance of the dynamics of the control system, simulations are made using matlab/simulink software. The results of the simulations concern a three-phase squirrel cage asynchronous motor with a power of 1.5 kW and with the parameters presented in table 2. Initially it was powered up and had a vacuum start. Then a load is applied at $t = 0.25s$.

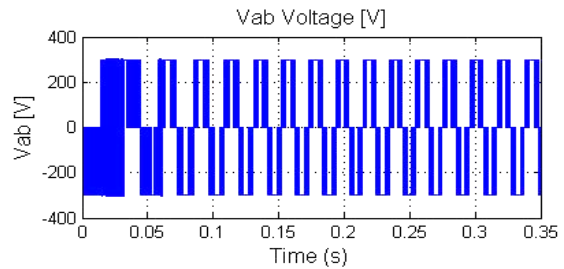


Figure 15. Line to line voltage of the inverter

The circuit produced a three-phase output ac voltage that had maximum voltage amplitude of the same value as the dc input voltage (figure 15). The behavior of the inverter at the output is checked.

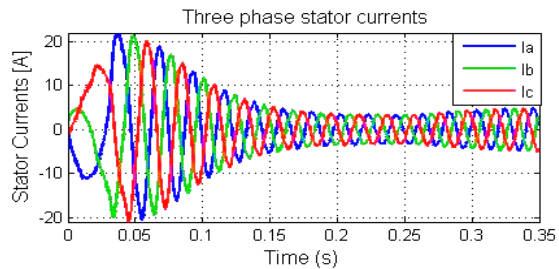


Figure 16. Three-phase stator currents (a, b, c)

The starting current of the motor is controlled at 4 times its nominal value and a reference of the progressive stator flux is applied (figure 16). The steady state of the stator current is reached around 0.15s, and then it stabilizes at its load value which is relatively large and very responsive but also reasonable since the engine is characterized by the presence of a significant air gap. The load is applied at $t = 0.25s$, the current reaches rapidly its stationary value (5.2 A).

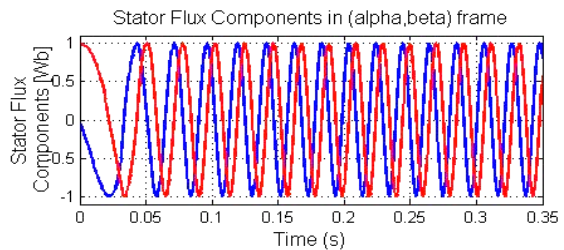


Figure 17. stator flux components (α, β) (Wb)

Figure 17 shows that the stator flux ripples are minimized, therefore the variations of the flux components are pure sinusoidal and their amplitudes are constant.

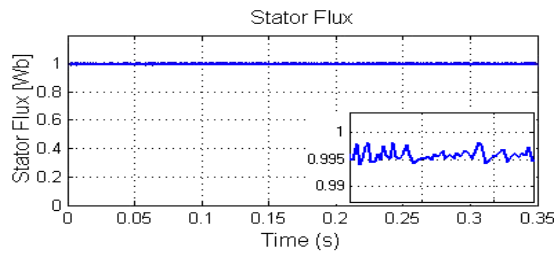


Figure 18. The stator flux (Wb)

Figure 18 shows the magnitude of the flux that is maintained at its reference, we can also note that it has a very low level of ripples.

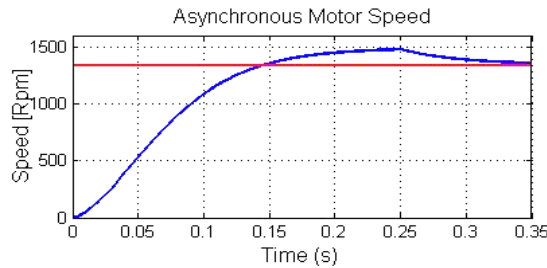


Figure 19. Asynchronous motor speed with load applied at 0.25s

Figure 19 illustrates the variation of speed; it quickly reaches the steady state whether it is unladen or after the application of the load and with a null static error, which proves the efficiency and robustness of the command.

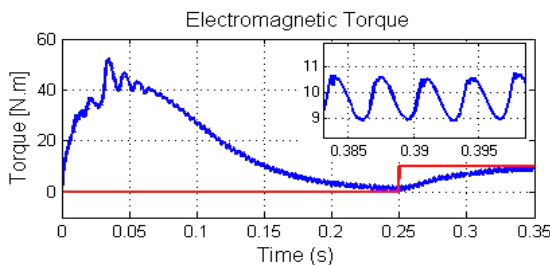


Figure 20. The electromagnetic torque with the load applied at 0.25s

It is found that the electromagnetic torque quickly reaches its maximum value which is beneficial to achieve a quick start, then returns to zero since it is unladen. When the load is applied, the motor reaches its operating point quickly with a delay not exceeding 0.1s. This proves the effectiveness of the control strategy.

➤ Switching on and start up on load:

The following figures (21-22-23) show the variations of the motor variables with a load start.

Figure 21 shows that the starting current does not exceed 4 times the nominal current and that the steady state is reached rapidly to 0.2s.

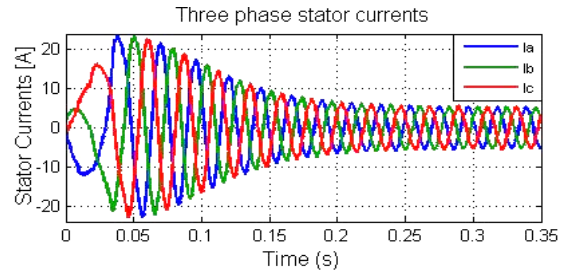


Figure 21. Three-phase stator currents (a, b, c)

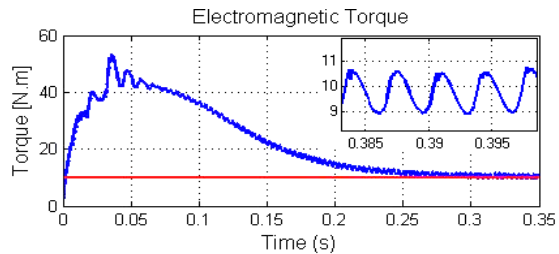


Figure 22. Electromagnetic torque

In figure 22, the torque quickly reaches its maximum value which allows a fast start of the motor, the steady state is obtained towards 0.25s. For the same reasons already mentioned, the torque has ripples around its instantaneous value. The speed (figure 23) quickly increases towards its reference.

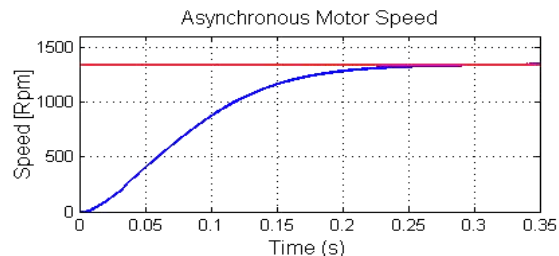


Figure 23. Motor speed

8. DISCUSSION

In order to demonstrate the efficiency of the proposed strategy, the system results were compared with some of the previous works in this field. The results show that using PI regulators instead of Hysteresis comparators in conventional DTC reduces ripples in stator flux and torque as the system is operating at constant switching frequency using the PWM modulator which decreases switching losses. The tuning process of PI controllers is done following the criteria adopted for electric drives such as optimal symmetry criterion and identification which achieved fast response and optimized system behavior with respect to disturbance signals. So according to the results from the previous works compared to this paper's work, the proposed strategy achieved good results.

Table 2: Engine and Regulator Parameters.

Parameters	Values
Motor type	1.5 Kw/ 50 Hz
Nominal current	6.4A
Stator resistance	4.85 Ω
Stator Inductance	0.274 H
Rotor Resistance	3.805 Ω
Rotor Inductance	0.274 H
Mutual Inductance	0.29 H
Moment of inertia	0.031 Kg.m ²
Friction factor	0.00114 N.m.s/rd
Stator flux	0.9960 Wb
P	2
Speed controller-K _p	2.943
Speed controller-K _i	69.94
Torque controller-K _p	1
Torque controller-K _i	211968.83
Flux controller-K _p	1e5
Flux controller-K _i	5e9
Sampling time	5 μ s

9. CONCLUSION

In this article, we studied the dynamics of speed, stator flux and torque of the three-phase asynchronous motor fed by a two-level inverter with sinusoidal PWM. The proposed scheme of direct torque and flux control was based solely on the analysis of stator equations such as conventional DTC, so the control algorithm is not sensitive to changes in rotor parameters, more known that the stator flux can be estimated from terminal quantities more precisely than the rotor flux. The closed loops presented in this proposed method was based on PI correctors which were tuned by using two types of setting methods such as identification and optimal symmetry criterion,

which allow us to improve significantly the system's control by reducing the response time and eliminating the static error. This strategy seems to be a good compromise between ease of implementation since it uses fewer control loops compared to other commands such as FOC "Field Oriented Control" and high performance since it increases the stability of speed and torque in the steady state and decreases the ripple of torque and stator flux compared to the conventional DTC control. The simulation results have proven the effectiveness and robustness of the entire control strategy.

REFERENCES:

- [1] W. Leonhard, "Controlled ac drives, a successful transition from ideas to industrial practice", Control Eng. Practice, Vol. 4, No. 7, 1996, pp. 897-908.
- [2] M. P. Kazmierkowski, R. Krishnan, F. Blaabjerg, "Control in power electronics selected problems", Academic Press, 2002.
- [3] R. Sadouni, A. Meroufel, "Performances comparative study of Field Oriented Control (FOC) and Direct Torque Control (DTC) of Dual Three Phase Induction Motor (DTPIM)", International Journal of Circuits, Systems and Signal Processing, Vol. 6, Issue 2, 2012.
- [4] I. Takahashi and T. Noguchi, "A new quick-response and high efficiency control strategy of an induction motor", IEEE Trans. on Ind. Applicat., Vol. IA-22, pp. 820-827, Sept./Oct. 1986.
- [5] D. Casadei, F. Profumo, G. Serra, A. Tani, "FOC and DTC: Two viable schemes for induction motors torque control", IEEE Transactions on Power Electronics, Vol. 17, No. 5, September 2002.
- [6] G. Didier "Modélisation et diagnostic de la machine asynchrone en présence de défaillances", Thèse de doctorat, Université Henri Poincaré, Nancy-I, 2003.
- [7] B. K. Bose, "Modern Power Electronics and AC Drives", Prentice Hall (I), 2007
- [8] F. Mehazzem, "Contribution à la commande d'un moteur asynchrone destiné à la traction électrique", Université Paris-Est, 2010.
- [9] C. Bajracharya, M. Molinas, J. Are Suul, T. M. Undeland, "Understanding of tuning techniques of converter controllers for VSC-HVDC", Nordic Workshop on Power and Industrial Electronics, June 9-11, 2008
- [10] M. Zelechowski, M. P. Kazmierkowski, F. Blaabjerg, "Controller design for direct torque controlled space vector modulated (DTC-

- SVM) induction motor drives”, IEEE ISIE 2005 Dubrovnik, Croatia, June 20-23, 2005.
- [11] M. P. Kazmierkowski, H. Tunia, “Automatic control of converter fed drives”, Elsevier Amsterdam-London-New York-Tokyo, 1994.
- [12] K. G. Papadopoulos, N. I. Margaritis, “Extending the Symmetrical Optimum criterion to the design of PID type-p control loops”, Journal of Process Control, 2011
- [13] X. Xu, R. De Doncker, D. W. Novomy, “A Stator Flux Oriented Induction Machine Drive”, Power Electronics Specialists Conference, 1988. PESC '88 Record, 19th Annual IEEE
- [14] Z. Qing, L. Zhihui, C. Jian, “A novel 3-phase SPWM technique: instantaneously floating the neutral point”, IEEE Power Electronics and Drive Systems, pp. 781-786, No. 2, Singapore, 1997.
- [15] Z. I. Çolak, E. Kabalcı, R. Bayındır, S. Sağiroglu, “The Design and Analysis of a 5-Level Cascaded Voltage Source Inverter with Low THD”, 9nd Power Engineering Energy and Electrical Drives Conference, Ankara, pp. 575-580, Lisbon, Portugal, March 18-20, 2009.
- [16] A. Kocalmis Bilhan, E. Akbal, “Modeling and simulation of two-level space vector PWM inverter using photovoltaic cells as DC source”, International Journal Of Electronics; Mechanical And Mechatronics Engineering Vol. 2 No. 4, pp. 311-317.
- [17] N. Tesla and D. H. Childress, “The fantastic inventions of Nikola Tesla: Adventures”, Unlimited Press, 1993.
- [18] D. B. Hoesason, “Squirrel-cage induction motors Electrical Engineers”, Journal of the Institution of, vol. 66, pp. 410-425, 1928.
- [19] A. Saghafinia, H. Wooi Ping, and M. Rahman, "High Performance Induction Motor Drive using Hybrid Fuzzy-PI and PI Controllers: a Review," International Review of Electrical Engineering-Iree, vol. 5, pp. 2000-2012, october-september 2010.
- [20] F. Blaschke, “A new method for the structural decoupling of A.C. induction machines”, in Conf. Rec. IFAC, Duesseldorf, Germany, pp. 1-15, October, 1971.
- [21] R. Toufouti S. Meziane, H. Benalla, “Direct Torque Control For Induction Motor Using Intelligent Techniques”, Journal of Theoretical and Applied Information Technology, Vol. 3, No. 3, pp. 35-44, 2007.
- [22] “Simple speed sensorless DTC-SVM scheme for induction motor drives”, Bulletin Of The Polish Academy Of Sciences Technical Sciences, Vol. 61, No. 2, 2013